

Pure bending creep of SUS 304 stainless steel tubes

Kuo-Long Lee†

Department of Mechanical Engineering, Far East College, Tainan, Taiwan, R.O.C.

Wen-Fung Pan‡

Department of Engineering Science, National Cheng Kung University, Tainan, Taiwan, R.O.C.

(Received September 18, 2002, Accepted November 7, 2002)

Abstract. This paper presents the experimental and theoretical results of SUS 304 stainless tubes with different diameter-to-thickness ratio (D/t ratio) subjected to pure bending creep. Pure bending creep occurs when a circular tube is bent to a desired moment and held at that moment for a period of time. It was found that the magnitudes of the creep curvature and ovalization of tube cross-section increase faster with a higher hold moment than that with a lower one. Due to continuously increasing curvature, the circular tubes eventually buckle. Finally, a theoretical form was proposed in this study so that it can be used to describe the relationship between the creep curvature and time. Theoretical simulations are compared with the experimental test data, showing that good agreement between the experimental and theoretical results has been achieved.

Keywords: pure bending creep; SUS 304 stainless steel tube; diameter-to-thickness ratio; creep curvature; ovalization.

1. Introduction

Understanding of the response and stability of long circular tubes subjected to bending is of importance in many industrial applications, such as structures in earthquake-prone area, offshore pipelines and platforms in extreme weather conditions, transporting tubes of heat exchangers for nuclear reactors or power plant, etc. It has been demonstrated that bending of circular tubes can lead to the ovalization of tube cross section, and this growth of ovalization causes a progressive reduction in tube bending rigidity. Eventually, when a critical value of the ovalization is reached, the tube buckles.

In recent years, studies have been made on circular tubes subjected to monotonic or cyclic pure bending with or without external pressure. Shaw and Kyriakides (1985) investigated the inelastic behavior of thin-walled tubes subjected to cyclic bending; Kyriakides and Shaw (1987) extended the analysis to the stability condition under cyclic bending; Corona and Kyriakides (1988) investigated the collapse of inelastic tubes subjected to combined bending and external pressure; Corona and Kyriakides

†Assistant Professor

‡Professor

(1991) discussed the degradation and buckling of circular tubes under cyclic bending and external pressure; Kyriakides and Ju (1992a, 1992b) experimentally and theoretically studied the bifurcation and localization instabilities of circular tubes under pure bending.

Subsequently, Pan *et al.* experimentally and theoretically investigated the response and stability of circular tubes subjected to monotonic or cyclic bending. Pan and Leu (1997) used endochronic theory to investigate the collapse of thin-walled tubes subjected to bending. The experimental data of 6061-T6 aluminum and 1018 steel tubes under cyclic bending tested by Kyriakides and Shaw (1985) were compared with the theoretical simulation. Pan *et al.* (1998) designed a new measurement apparatus, which can be placed at the mid-span of the circular tube specimen and is suitable for simultaneous experimental determinations of the tube curvature and ovalization of the tube cross-section. Pan and Fan (1998) investigated the effect of prior curvature-rate in the preloading stage on the subsequent creep or relaxation behavior. It has been found that the curvature-rate at the preloading stage has a strong influence on the subsequent creep or relaxation deformation under pure bending. Pan and Her (1998) investigated the response and stability of 304 stainless steel tubes subjected to cyclic bending with different curvature-rates. They discovered that higher applied curvature-rates indicate greater hardening of tubes. However, the ovalization of tube cross-section increases when the applied curvature-rate increases. Pan and Hsu (1999) experimentally and theoretically studied the viscoplastic behavior of 304 stainless steel tubes subjected cyclic bending. The endochronic viscoplastic theory, which was proposed by Pan and Chern (1997), was used to investigate the viscoplastic behavior of the tubes under cyclic bending. Lee and Pan (2001) experimentally and theoretically investigated the viscoplastic response and stability of titanium alloy tubes subjected cyclic bending. The theoretical formulation, proposed by Pan and Her (1998), was modified so that it could be used to simulate the relationship between the controlled curvature and the number of cycles to produce buckling for titanium alloy tubes under cyclic bending with different curvature-rates. Lee *et al.* (2001) discussed the influence of the diameter-to-thickness ratio to the response and stability of circular tubes subjected to symmetrical cyclic bending. The empirical relationship, proposed by Kyriakides and Shaw (1987), was modified so that it can be used for simulating the relationship between the controlled curvature and the number of cycles to produce buckling for circular tubes with different D/t ratio.

In this paper, the response of SUS 304 stainless steel tubes with different diameter-to-thickness ratio (D/t ratio) under pure bending creep is studied. In such a test the tube is bent to a certain amount of moment and held for a period of time. A four-point bending machine (Pan *et al.* 1998, Pan and Her 1998, Pan and Fan 1998, Pan and Hsu 1999, Lee *et al.* 2001) was used to conducting the tests. The curvature-ovalization measurement apparatus, designed by Pan *et al.* (1998), was used to measure the magnitudes of the tube curvature and the ovalization of the tube cross-section. The creep process was controlled by load cells, mounted in the bending machine. Since the phenomenon of pure bending creep is very similar to the phenomenon of uniaxial creep, a theoretical form, which is similar to the formulation of the uniaxial creep, was proposed so that it could be used to simulate the relationship between the creep curvature and time.

2. Bending test facilities

In this study, a bending test facility, consisting of a pure bending device and a curvature-ovalization measurement apparatus, was used for a number of experiments on circular tubes under pure bending creep. The test facility is further described below.

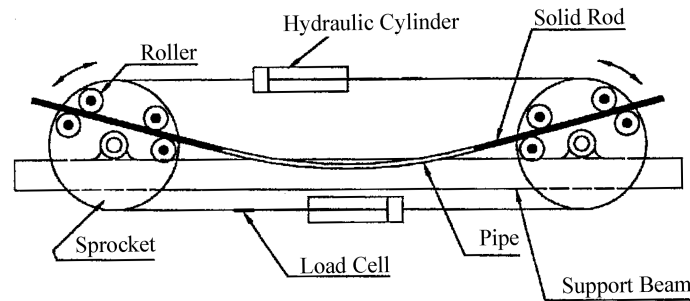


Fig. 1 A schematic drawing of the bending device

2.1. Pure bending device

Fig. 1 shows a schematic drawing of the bending device, which was designed as a four-point bending machine. The device consists of two rotating sprockets, about 30 cm in diameter, symmetrically resting on two support beams of 1.25 m apart. The maximum length of the test specimen was 1 m. The two sprockets support two rollers which apply point loads as a couple at each end of the test specimen. Heavy chains run around these sprockets and are connected to two hydraulic cylinders and load cells forming a closed loop. Once either the top or bottom cylinder contracts, the sprockets rotate, and pure bending of the test specimen is achieved. The contact between the tube and the rollers is free to move along axial direction during bending. The load transfer to the test specimen is in the form of a couple formed by concentrated loads from the two rollers. A servo-hydraulic, feedback control system was developed to prescribe cyclic loading histories. The output from either the curvature-ovalization measurement apparatus or from the load-cell can be selected as feedback for curvature or moment control, respectively. A detailed description of such a bending device can be found in literature (Kyriakides and Shaw 1987, Corona and Kyriakides 1991, Pan *et al.* 1998, Pan and Hsu 1999).

2.2. Curvature-Ovalization Measurement Apparatus (COMA)

Fig. 2 shows a schematic drawing of the COMA. It is a lightweight instrument which can be mounted close to the tube's mid-span (Pan *et al.* 1998). It can be used to monitor the changes in the major and minor diameters of the tube cross-section, using a magnetic detector (middle part of the COMA). Simultaneously, it can be used to measure variations in the tube curvature close to the mid-span from the signals of inclinometers. There are three inclinometers in the COMA. Two of them are fixed on two holders, (see Fig. 2). The holders are fixed on the circular tube before the test begins, and the angles of rotation detected by these two side-inclinometers are in the plane which is the direction of the bending moment. Once the two holders are placed and fixed on the circular tube, the distance between the two side-inclinometers is fixed, and denoted as L_o . Consider that the circular tube is subjected to pure bending, the angle changes detected by the two side-inclinometers are denoted as θ_1 and θ_2 (see Fig. 3). Due to the uniform bending in all sections, the circular tube, which was originally straight, is deformed into a circular arc. The distance between the center of this arc and the neutral surface is denoted as ρ (shown in Fig. 3). From Fig. 3, the value of L_o is determined as

$$L_o = \rho (\theta_1 + \theta_2) \quad (1)$$

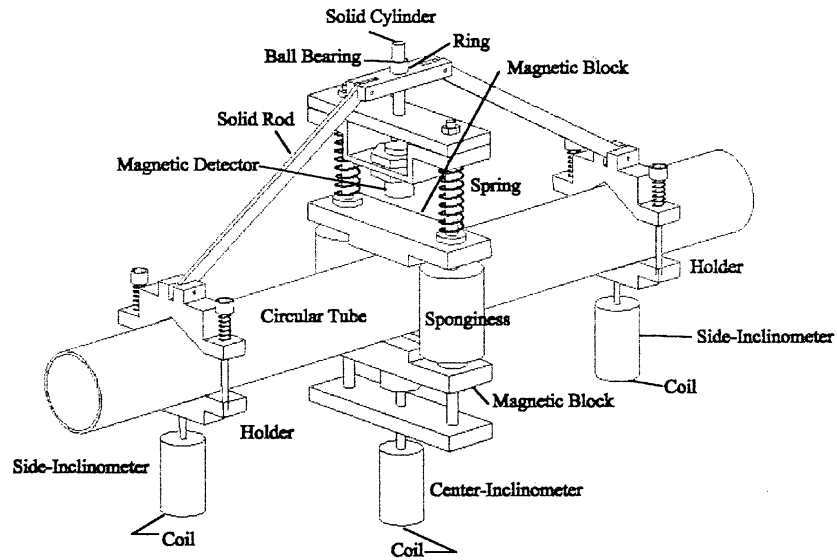


Fig. 2 A schematic drawing of the COMA

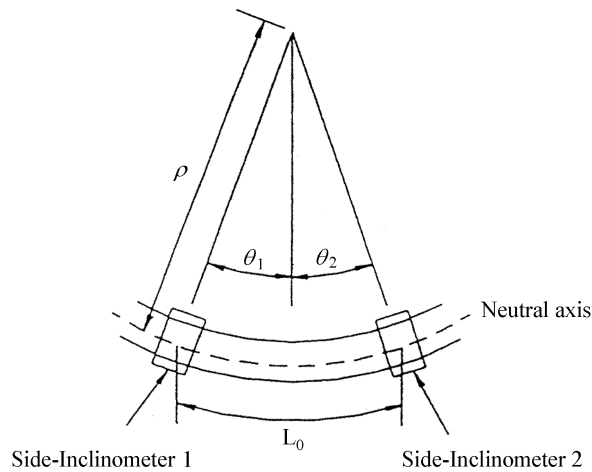


Fig. 3 Tube deformation between two side-inclinometers under pure bending

The curvature of the tube κ is

$$\kappa = \frac{1}{\rho} = \frac{(\theta_1 + \theta_2)}{L_o} \quad (2)$$

Once the distance between the two side-inclinometers (L_o) is fixed and the angle changes (θ_1 and θ_2) of the two side-inclinometers are detected, the curvature of the tube can be determined from Eq. (2). Thus, the COMA can provide a direct measurement of the tube curvature.

3. Material and experimental procedures

In this section, we discuss the specimens and the test procedures of circular tubes subjected to pure bending creep. Specimens and the test procedures are given below:

3.1. Material and specimens

The material used in this study was hot-rolled SUS 304 stainless steel circular tubes with the chemical composition of Cr 18.36, Ni 8.43, Mn 1.81, Si 0.39, C 0.05, P 0.28, S 0.04, and the remainder Fe. The yield stress is 205 MPa, the tensile ultimate stress is 520 MPa and the percent elongation is 35%. The test specimens originally had a nominal outside diameter D of 38.1 mm and a wall thickness t of 1.5 mm ($D/t = 25.4$). To obtain the desired D/t ratio, the as-received tubes were slightly machined on the outside surface. The magnitudes of the D/t ratio were selected to be 60, 50, 40 and 30 in this study. Fig. 4 shows the dimensions of four different D/t ratios of tested tubes.

3.2. Pure bending creep procedures

The pure bending creep test was conducted by using the bending device described in the previous section. The magnitude of the curvature was controlled and measured by the COMA, which also measured the ovalization of tube cross-section. The bending moment can be calculated from the signals detected by the two load cells, mounted on the bending device. For pure bending creep test, the

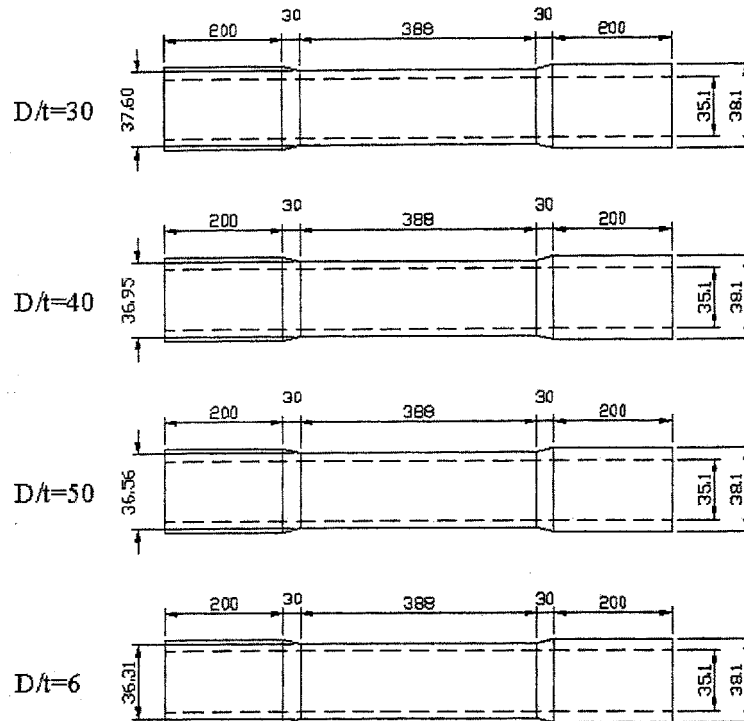


Fig. 4 Dimensions of four different D/t ratios of SUS 304 stainless steel tubes

specimen was bent in a curvature-controlled mode (controlled by the COMA) at the preloading stage while the computer monitored the magnitude of the moment. As soon as the moment magnitude reached the preset creep hold moment, the loading process was stopped. The test system was programmed to switch to the moment-controlled mode (controlled by the load cells) and the moment was kept at this constant magnitude, while the tube curvature and ovalization of tube cross-section were being recorded.

4. Experimental result

4.1. Pre-creep stage

Fig. 5 presents the moment (M) - curvature (κ) responses for SUS 304 stainless steel tubes with $D/t = 30, 40, 50$ and 60 subjected to pure bending at pre-creep stage. For each D/t ratio, a linear moment-curvature curve is observed when the bending moment is in the elastic range. Once the deformation is in the plastic range, the moment-curvature curve becomes nonlinear. Fig. 6 shows the corresponding results for ovalization of tube cross-section as a function of the applied curvature. The ovalization of tube cross-section is defined by $\Delta D/D$, where D is the outside diameter and ΔD is the change in the outside diameter. It can be noted that the ovalization of tube cross-section increases when the applied curvature increases.

4.2. Creep stage

Fig. 7 depicts a typical drawing of the curvature (κ) - time (t) profiles of the overall bending process (the pre-creep and the creep stages) for circular tubes with $D/t = 60$. Four different magnitudes of the hold moment, i.e., 130, 150, 170 and 190 N-m, were controlled for circular tubes subjected to pure

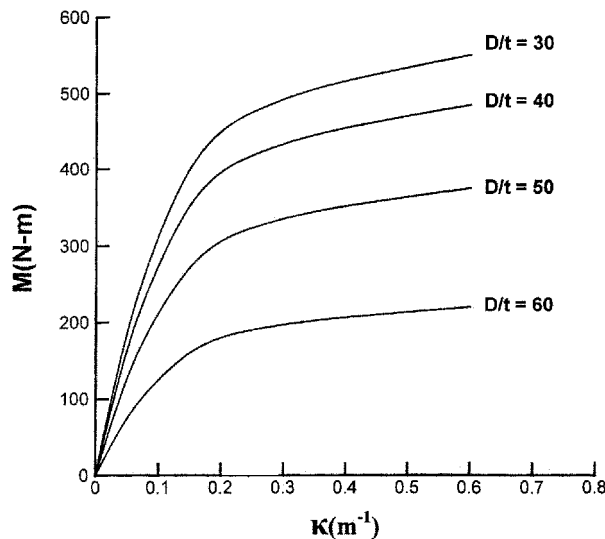


Fig. 5 Experimental moment (M) curvature (κ) curves under pure bending for various D/t ratios

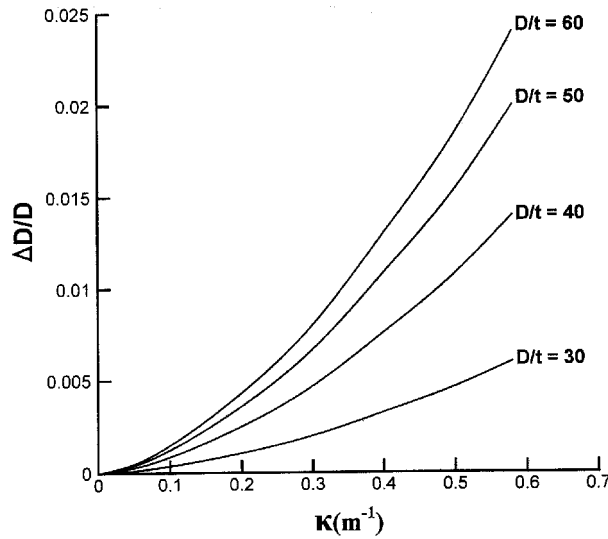


Fig. 6 Experimental ovalization ($\Delta D/D$) curvature (κ) curves under pure bending for various D/t ratios

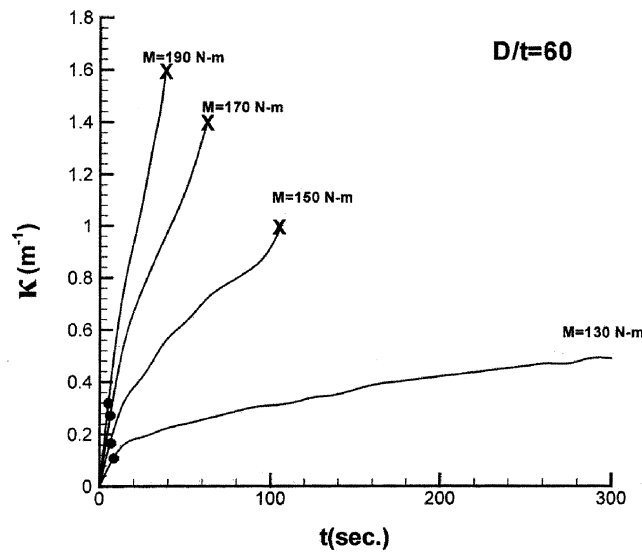


Fig. 7 Experimental curvature (κ) time (t) curves under pure bending creep for four different hold moments with $D/t = 60$ (“•” and “×” denote the starting and buckling points of the creep stage, respectively)

bending creep. The starting and buckling points of the creep response are marked by “•” and “×”, respectively. Due to the much longer time at buckling (954 seconds) under hold moment of 130 N-m, the buckling point at the curvature-time curve is not indicated in Fig. 7. It can also be seen from Fig. 7 that the magnitudes of the creep curvature at buckling for these four hold moments are different. The curvature at buckling with a higher hold moment is larger than that with a smaller hold moment.

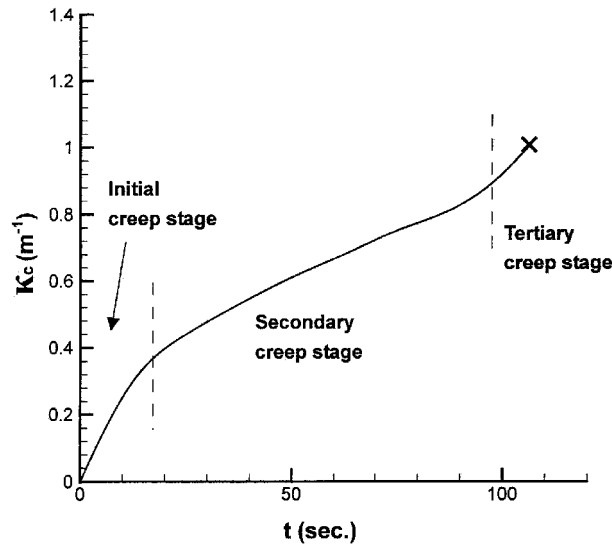


Fig. 8 Experimental creep curvature (κ_c) time (t) curve under pure bending creep for hold moment of 170 N-m and $D/t = 60$ ("X" denote the buckling point of the creep stage)

We consider the creep stage of Fig. 7 from the starting point "•" to buckling point "X". A typical result of the creep curvature (κ_c) - time (t) curve for tube with $D/t = 60$ and the hold moment = 170 N-m under pure bending creep is shown in Fig. 8. It can be observed that the creep process has three stages: initial, secondary and tertiary creep stages. It can also be seen that once pure bending creep starts, the magnitude of the curvature increases (the initial creep stage). However, the rate of creep gradually decreases. Thereafter, the pure bending creep enters the secondary creep stage. In this stage, the creep curvature increases steadily with time and the creep curvature-rate is approximately constant. The final portion of the pure bending creep is called the tertiary creep stage. In this stage, the creep curvature-rate increases drastically and buckling of the tube occurs. It was also found that the larger magnitude of the moment, the faster the creep curvature increases. Due to the continuously increasing curvature during the pure bending creep, the circular tubes eventually buckle.

Fig. 9 demonstrates the corresponding ovalization ($\Delta D/D$) - time (t) curves of the whole loading process under four different magnitudes of hold moment (the pre-creep stage and the creep stage). The starting and buckling points of the pure bending creep are also marked by "•" and "X", respectively. It can be observed that the initial ovalization-rate of the pure bending creep with a higher hold moment is larger than that of the pure bending creep with a smaller hold moment. However, the ovalizations at buckling for these four magnitudes of hold moment are almost the same. It also can be noted that due to the much longer time at buckling for hold moment of 130 N-m, the buckling point at the ovalization-time curve is not indicated in Fig. 9. To highlight the influence of the D/t ratio to the response and stability under pure bending creep, circular tubes with $D/t = 50, 40$ and 30 were also tested. The phenomenon of the curvature (κ) - time (t) curves and ovalization ($\Delta D/D$) - time (t) curves was found to be very similar to the phenomenon of a circular tube with $D/t = 60$.

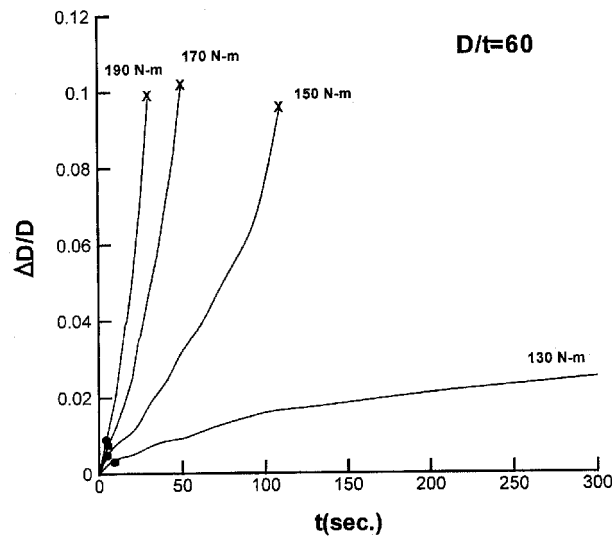


Fig. 9 Experimental ovalization ($\Delta D/D$) time(t) curves under pure bending creep for four different hold moments with $D/t = 60$ ("•" and "x" denote the starting and buckling points of the creep stage, respectively)

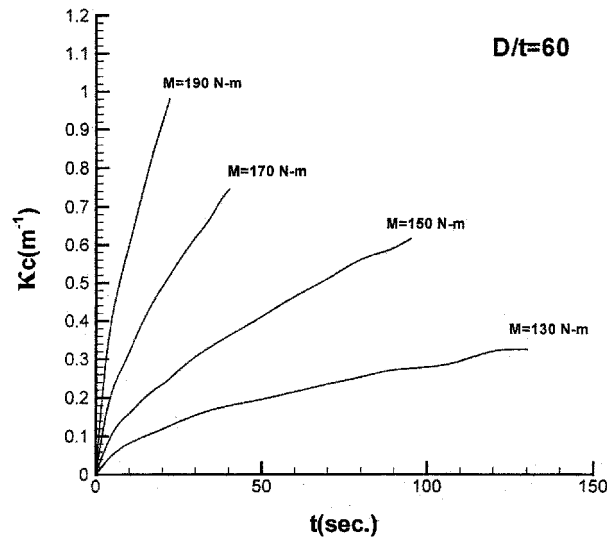


Fig. 10 Experimental result of creep curvature(κ_c) vs. time(t) curves at initial and secondary stages for $D/t = 60$

5. Discussion

In this study, a theoretical form is proposed for simulating the relationship between the creep curvature and time for circular tubes with different D/t ratios subjected to pure bending creep. Because most of the time for the pure bending creep is spent in the initial and secondary creep stages, the proposed form is only applicable in these two stages. Fig. 10 shows the creep curvature (κ_c) - time (t) curve for SUS 304 stainless steel circular tube with $D/t = 60$ in the initial and secondary creep stages. In addition, the creep curvature (κ_c) - time (t) curves for $D/t = 50, 40$ and 30 in the initial and secondary

creep stages have similar trend as the tubes with $D/t = 60$. The experimental results are shown in Figs. 13-15. Since the trend of the creep curvature-time curve for pure bending creep is very similar to the trend of creep strain-time curve for uniaxial creep, the formulation for creep strain-time curve under uniaxial creep can be modified so that the formulation can be used to simulate the creep curvature-time curve under pure bending creep. In this study, the Bailey-Norton law used for the uniaxial creep is considered, formulated as

$$\varepsilon_c = C \sigma^m t^n \quad (3)$$

where ε_c is the creep strain, σ is the hold stress for uniaxial creep, and C , m and n are material parameters. For pure bending creep, a similar form is proposed as

$$\kappa_c = C M^m t^n \quad (4)$$

where κ_c is the creep curvature, M is the hold moment for pure bending creep, and C , m and n are material parameters, which are related to the material properties and the D/t ratio.

By curve fitting with the experimental data of SUS304 stainless steel tubes with $D/t = 60, 50, 40$ and 30 , the magnitudes of m and n for these four D/t ratios are approximately 5.7 and 0.53 , respectively. However, the material parameters C for $D/t = 60, 50, 40$ and 30 are 1.93×10^{-14} , 4.71×10^{-16} , 3.92×10^{-17} and 8.67×10^{-18} , respectively. If we consider the relationship between $\log C$ and $(D/t)^3$, a straight line can be used to described the relationship (see Fig. 11). Therefore, parameter C , which is related to the material properties and the D/t ratio, is proposed to be

$$\log C = a \left[\frac{D}{t} \right]^3 + b \quad (5)$$

where a and b are material parameters which can be determined from Fig. 11. By using the least square method, the parameters a and b are determined from Fig. 10 to be 1.77×10^{-5} and $b = -17.54$,

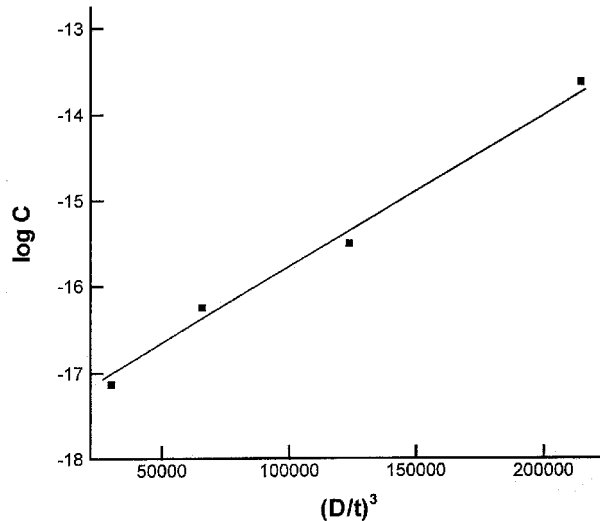


Fig. 11 The relationship between $\log C$ and $(D/t)^3$

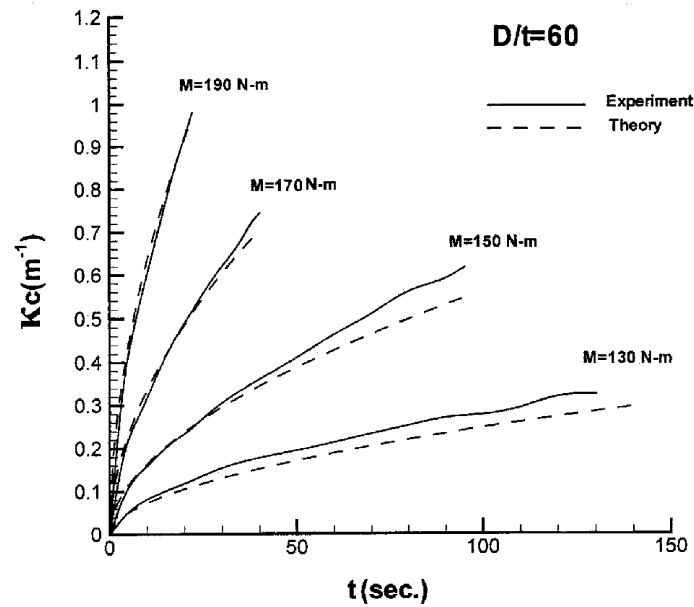


Fig. 12 Experimental and theoretical results of creep curvature(κ_c) vs. time(t) curves at initial and secondary stages for $D/t = 60$

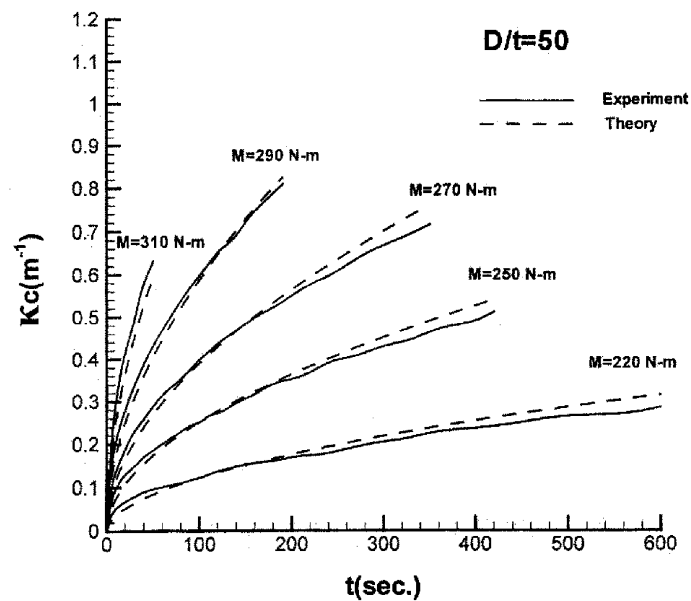


Fig. 13 Experimental and theoretical results of creep curvature(κ_c) vs. time(t) curves at initial and secondary stages for $D/t = 50$

respectively. The experimental data and simulated results for 304 stainless steel circular tubes with $D/t = 60, 50, 40$ and 30 are demonstrated in Figs. 12-15 by the solid and dashed lines, respectively. Good agreement between the experimental and theoretical results has been achieved.

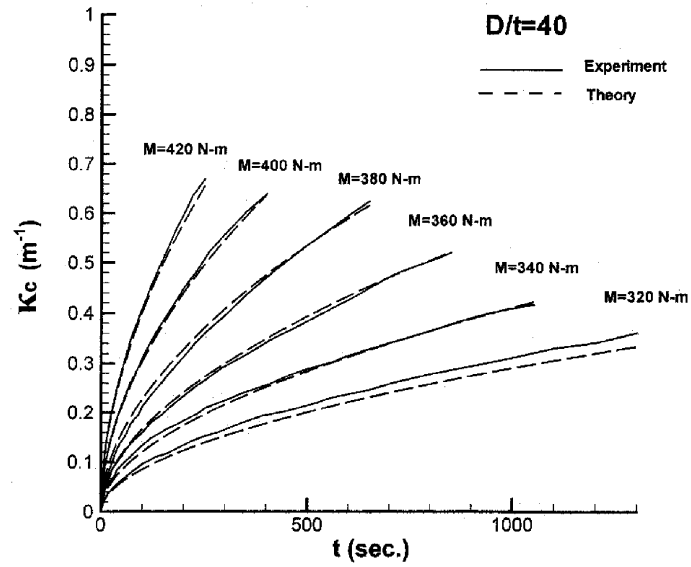


Fig. 14 Experimental and theoretical results of creep curvature(κ_c) vs. time(t) curves at initial and secondary stages for $D/t = 40$

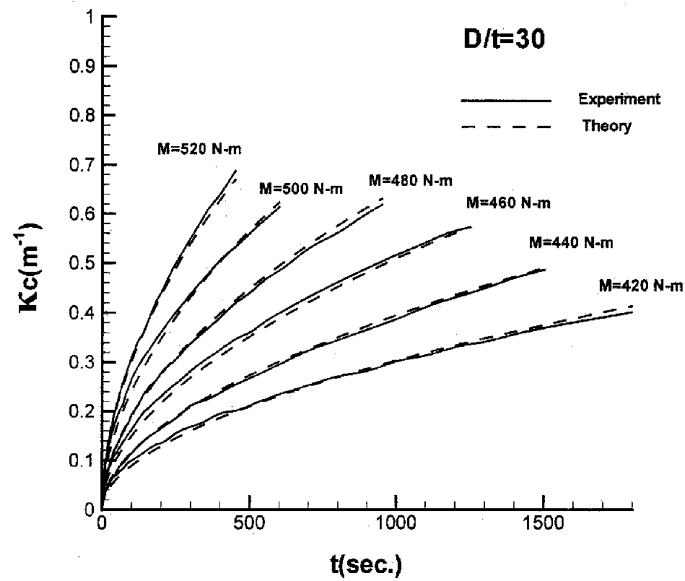


Fig. 15 Experimental and theoretical results of creep curvature(κ_c) vs. time(t) curves at initial and secondary stages for $D/t = 30$

6. Conclusions

The case of circular tubes under pure bending creep was investigated in this study. A pure bending device and the COMA were used to test the circular tubular specimens for 304 stainless steel with

different D/t ratio under pure bending creep. The following conclusions can be drawn from this investigation:

- (1) It can be observed from the creep curvature vs. time curves that the loading process can be divided into three stages, the initial, secondary and tertiary creep stages. Once creep starts, the magnitude of the tube curvature increases during the initial creep stage. But thereafter, the tube enters a secondary creep stage, when the curvature increases steadily with time. In the tertiary creep stage, the increase in creep curvature-rate is large, and the tube buckles eventually.
- (2) The creep curvature-rate is larger with a higher hold moment than that for a lower one. In addition, the magnitudes of creep curvature at buckling for these four holding moments are different. The curvature at buckling with a higher hold moment is larger than that with a smaller hold moment.
- (3) From the ovalization vs. time curves for circular tubes subjected to pure bending creep, it was found that the ovalization of tube cross-section increases steadily at the initial and secondary stages. However, the ovalization of tube cross-section increases quickly with time at the tertiary creep stage. Furthermore, the creep ovalization-rate of tube cross-section is larger with a higher hold moment than that with a lower one.
- (4) A form of the creep curvature and time for circular tubes with different D/t ratio subjected to pure bending creep was proposed as Eq. (4). It is noted that the form is applicable only at the initial and secondary creep stages. It is shown that theory can adequately simulate the experimental results (see Figs. 12-15).

Acknowledgements

The work presented was carried out with the support of National Science Council under grant NSC 88-2212-E-006-016. Its support is gratefully acknowledged

References

- Corona, E., Kyriakides, S. (1988), "On the collapse of inelastic tubes under combined bending and pressure", *Int. J. Solids Struct.*, **24**(5), 505-535.
- Corona, E., Kyriakides, S. (1991), "An experimental investigation of the degradation and buckling of circular tubes under cyclic bending and external pressure", *Thin-Walled Struct.*, **12**, 229-263.
- Kyriakides, S., Ju, G.T. (1992a), "Bifurcation and localization instabilities in cylindrical shells under bending", - I. Experiments. *Int. J. Solids Struct.*, **29**(9), 1117-1142.
- Kyriakides, S., Ju, G.T. (1992b), "Bifurcation and localization instabilities in cylindrical shells under bending", - II. Predictions. *Int. J. Solids Struct.*, **29**(9), 1143-1171.
- Kyriakides, S., Shaw, P.K. (1987), "Inelastic buckling of tubes under cyclic loads", *J. Press. Vessel Technol.*, ASME, **109**, 169-178.
- Lee, K.L., Pan, W.F. (2001), "Viscoplastic collapse of titanium alloy tubes under cyclic bending", *Int. J. Struct. Engng. Mech.*, **11**(3), 315-324.
- Lee, K.L., Pan, W.F., Kuo, J.N. (2001), "The influence of the diameter-to-thickness ratio on the stability of circular tubes under cyclic bending", *Int. J. Solids Struct.*, **38**, 2401-2413.
- Pan, W.F., Chern, C.H. (1997), "Endochronic description for viscoplastic behavior of materials under multiaxial loading", *Int. J. Solids Struct.*, **34**(17), 2131-2159.
- Pan, W.F., Fan, C.H. (1998), "An experimental study on the effect of curvature-rate at preloading stage on

- subsequent creep or relaxation of thin-walled tubes under pure bending”, *International Journal, Series A.*, JSME, **41**(4), 525-531.
- Pan, W.F., Her, Y.S. (1998), “Viscoplastic collapse of thin-walled tubes under cyclic bending”, *J. Engng. Mat. Tech.*, ASME, **120**, 287-290.
- Pan, W.F., Hsu, C.M. (1999), “Viscoplastic analysis of thin-walled tubes under cyclic bending”, *Int. J. Struct. Engng. Mech.*, **7**(5), 457-471.
- Pan, W.F., Leu, K.T. (1997), “Endochronic analysis for viscoplastic collapse of thin-walled tube under combined bending and external pressure”, *International Journal, Series A.*, JSME, **40**(2), 189-199.
- Pan, W.F., Wang, T.R., Hsu, C.M. (1998), “A curvature-ovalization measurement apparatus for circular tubes under cyclic bending”, *Experimental Mechanics-an International Journal*, **38**(2), 99-102.
- Shaw, P.K., Kyriakides, S. (1985), “Inelastic analysis of thin-walled tubes under cyclic bending”, *Int. J. Solids Struct.*, **21**(11), 1073-1110.

CC